SciEn
Journal of Engineering Advancements Vol. 04(02) 2023, pp 35-39 https://doi.org/10.38032/jea.2023.02.001

Fault Diagnosis in Gas Lift System Using PDF Data

Ojonugwa Adukwu

Department of Industrial and Production Engineering, School of Engineering and Engineering Technology, Federal University of Technology, P.M.B.704, Akure, Ondo State, Nigeria

Received: June 03, 2023, Revised: June 13, 2023, Accepted: June 14, 2023, Available Online: June 25, 2023

ABSTRACT

Fault detection and isolation in the gas lift system were implemented assuming the gas lift variables are stochastic. Injection valve coefficient (C_{iv}), production choke coefficient (C_{pc}), annulus pressure (P_a), and wellhead pressure (P_{wh}) were observed to show variations with faults presence. By simulating these gas lift variables as stochastic, the probability density function (PDF) data were used to generate decision functions for both the detection and isolation of the gas lift valve faults. The scheme accurately detected and isolated faults in the injection valve coefficient (C_{iv}) and production choke coefficient (C_{pc}). The result of this diagnosis will aid the proper implementation of fault tolerant control in the gas lift system which will lead to its optimal operation.

Keywords: Gas Lift, Fault Detection, Fault Diagnosis, Fault Isolation, PDF Data.

1 Introduction

Gas lift systems are used for lifting crude oil into the production platforms when the reservoir pressure becomes insufficient [1]-[3]. Due to the location and the materials transported, gas lift usually suffers from faults that reduce its ability to function as desired or even cause danger. To optimally operate the gas lift system, therefore, a proper fault diagnosis procedure must be implemented.

Fig. 1 is a gas lift system. The key variables are the pressures, flow rates, and masses. The pressures are annulus pressure (P_a), reservoir pressure (P_r), bottomhole pressure (P_{bh}), well pressure (P_w), wellhead pressure (P_{wh}) and separator pressure (P_s). The flow rates are flow of lift gas from the compressor into the annulus (w_{gl}), flow from annulus into tubing (w_{iv}), flow from reservoir into the tubing (w_r) and flow from the tubing into the separator (w_{pc}). The masses are the mass of gas in the annulus (m_{ga}), mass of gas in tubing (m_{gt}) and mass of oil in tubing (m_{ot}). These masses form the states of the gas lift system.

The natural source of energy for the lift is the reservoir pressure (P_r) [4]-[5]. During the operation of the system, this pressure could become insufficient to lift the crude as desired. Gas from the compressor station is therefore supplied to the annulus through the gas lift valve. The gas then flows to the tubing through the injection valve and mixes with the liquid in the tubing. This lightens the tubing liquid ensuring adequate oil production again [6]-[7].

The valves control the flow of oil through the system [8]-[9]. The opening and closing of the valves expose the valves to faults that affect their optimal operation. Due to the variation of reservoir parameters in particular, the gas/oil ratio (GOR), the gas lift variables are stochastic in nature, and fault diagnosis using the variables is better implemented using probability density function (PDF) data similar to results in DC motor in [10].

In this article, faults in gas lift valves are detected and isolated. Variables that change in response to faults presence are selected. The residuals which follow Gaussian distribution hence permit the use of the PDF data to provide the decision functions presented. The decision functions to detect the fault are monitored. By generating fault signatures, the faults are isolated.

The remainder of this article is as follows: Section 2 discusses the materials and methods; Section 3 presents the results and discussion, and Section 4 concludes the article.

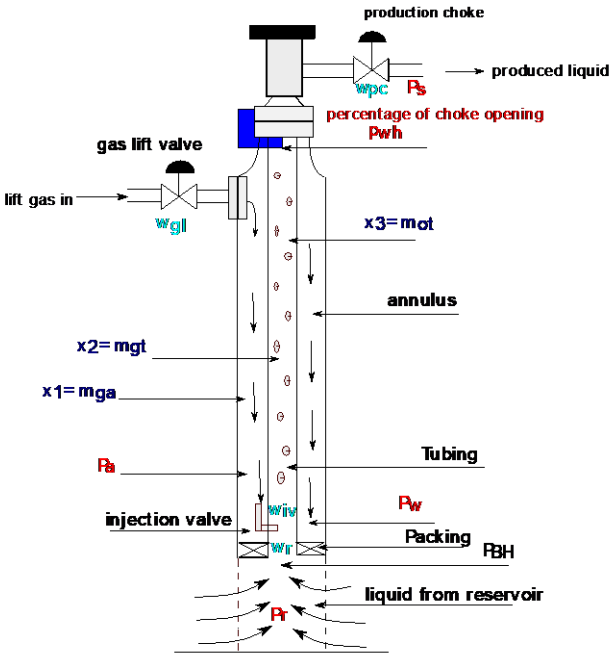

Fig. 1 A single-well gas lift system

2 Materials and Methods

2.1 Gas Lift faults

Fault diagnosis involves three activities namely: (i) detection, (ii) isolation, and (iii) identification. While fault detection implies detecting fault presence, fault isolation involves determining faulty components and fault isolation deals

*Corresponding Author Email Address: oaualaku@yahoo.co.uk

with identification of fault type. Some valve faults can have a step-change effect on the flow rate. The valve coefficient is obtained by lumping together all the constants that affect flow rates through the valve. For a fluid of constant density at a given temperature, C_{iv} is the flow rate per unit pressure change (ΔP) if the percentage valve opening is constant. Hence, the flow rate through the valve is determined by the valve coefficients as well as the percentage of valve opening if the pressure, density, and temperature are fixed. Faults have effects on the control of flow rate using the valve coefficients as parameters.

Fault diagnosis is therefore implemented here by assuming valve faults to result in a step-like change in these valve coefficients. The other assumption is that the gas lift variables are Gaussian implying zero mean with nonzero variance.

Augmented states are therefore obtained if the valve coefficients are added to the masses described in section 1 as:

$$x = [m_{ga} \quad m_{gt} \quad m_{ot} \quad C_{iv} \quad C_{pc}]^T \qquad (1)$$

These augmented states vary for m_{ga}, m_{gt}, m_{ot} but remains constant for C_{iv}, C_{pc} until the arrival of faults.

2.2 Gas Lift Variables Used for Fault Detection

Fault detection involves generating a residual, r. This residual is constant at a steady state at each time sample in the absence of fault. This is still true even in the presence of input change and disturbance for an ideal system. This residual changes only when there is a fault. For a stochastic system, with Gaussian noise distribution, the residual has zero mean and nonzero variance. At no-fault case. The mean is however nonzero at all or some points when there is fault.

C_{iv} and C_{pc} are good candidates to be used to generate fault signatures. Other variables also vary in known ways due to faults in the valves. Fig. 2 shows an abrupt fault of 20% step increase in C_{iv} introduced at the 60th minute and C_{pc} introduced at the 120th minute while Fig. 3 shows the step decrease.

In Fig. 2 and Fig. 3 a step fault in C_{iv} has no affect C_{pc}, similarly, a step fault in C_{pc} does not affect C_{iv}. Therefore, if a residual is generated for a fault in the C_{iv}, it will not affect the residual for the fault in the C_{pc}. To improve detection and isolation, we increase the number of variables that will be used to generate fault signatures. We make an assumption to enable us to use this: there is no disturbance input and the system is operating at a steady state where the control input is constant throughout. Removing the disturbance effect helps avoid having to solve the optimization problem to decouple the disturbance effect hence easing our fault detection here. We, therefore, add other variables to the two gas lift valve coefficients. These additional variables are discussed briefly below:

P_a: The pressure in the annulus is directly affected by the injection valve coefficient (C_{iv}). All other things being constant, P_a decreases if C_{iv} increases owing to more gas flow from the annulus into the tubing which decreases the mass of gas in the annulus m_{ga}. But P_a is affected by other variables namely, the pressure in the well at the injection point (P_w) and the rate of gas injection into the annulus (w_{gl}). Despite these a change in C_{iv} will show symptoms in P_a hence it is selected as one of the variables for detection to a large extent. But since annulus pressure is also affected by the well pressure at the injection point, P_a is also affected by w_{pc} since it affects the P_w.

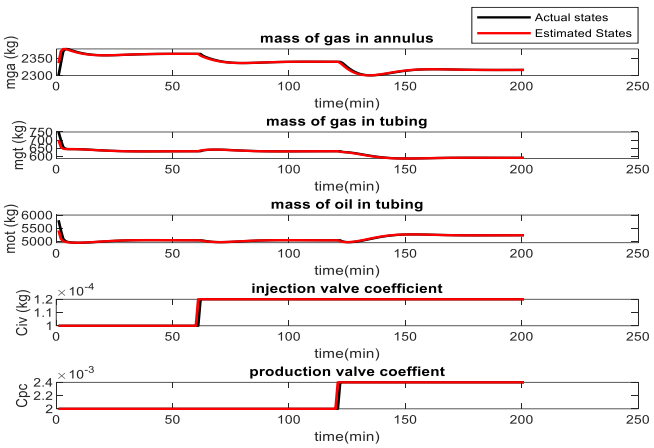

Fig. 2 Augmented gas lift states with a 20 % step increase in valve coefficients

Consequently, a fault in C_{iv} and C_{pc} show symptoms in P_a if a disturbance is removed and the system operates at constant input. This is shown where in both cases, the residual responded in the same way to fault presence, hence this is used for fault detection.

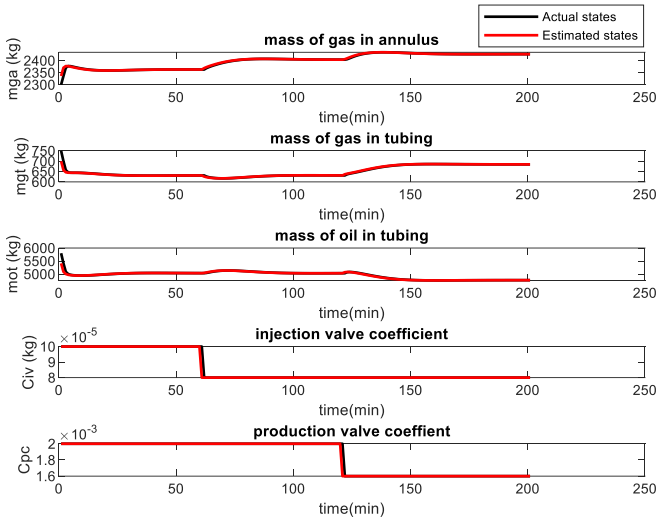

Fig. 3 Augmented gas lift states with a 20 % step decrease in valve coefficients

P_{wh}: The pressure of the wellhead is affected by the flow rate through the production choke w_{pc}. The pressure decreases as the production rate increases. P_{wh} depends on the mass of tubbing gas which is contributed by flow from the reservoir and from the annulus. P_{wh} is hence affected by C_{iv} too but minimally as the loss in mass due to reduced w_{iv} can be compensated for by the flow from the reservoir. A fault in C_{iv} shows little effect on the P_{wh} as seen in Fig. 4(b) where the fault in C_{iv} affected the residual only during the fault transient period. A fault in C_{pc} shows strong effect on P_{wh} as shown in Fig. 5(b). P_{wh} can therefore be used for both detection and isolation when appropriate threshhold is selected.

Flowrates: Many other variables vary in an observable way with valve coefficients faults when the disturbance is ignored and input kept constant; for example, Fig. 6 shows the flow rates for the gases.

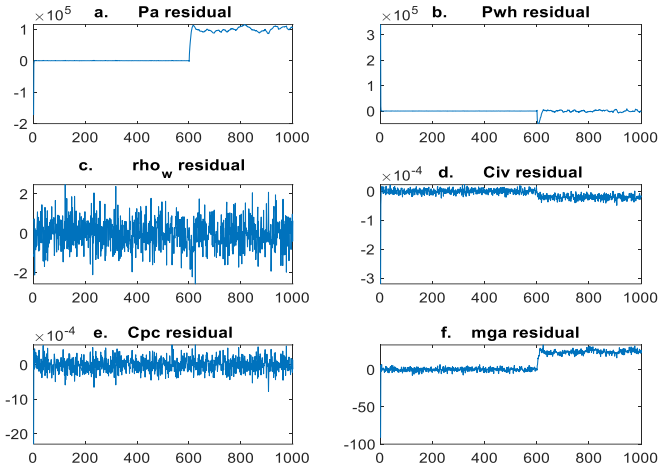

Fig. 4 Gas lift residual with a 20 % step increase in C_{iv}

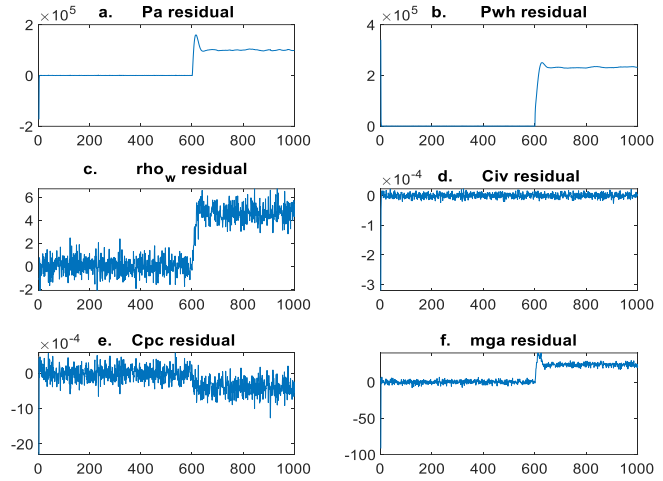

Fig. 5 Gas lift residual with a 20 % step increase in C_{pc}

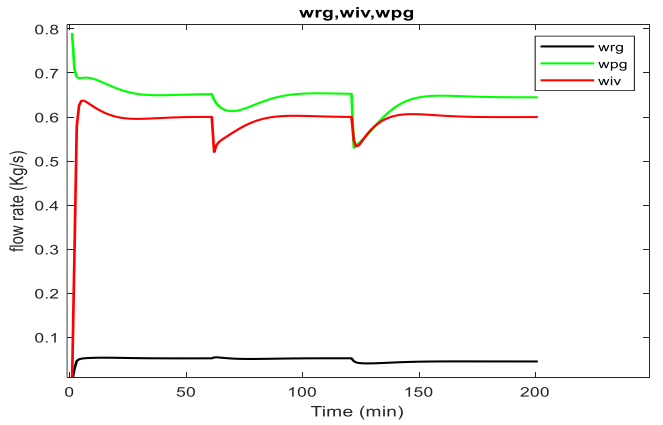

Fig. 6 Gas lift residual with a 20 % step increase in C_{pc}

Both w_{rg} and w_{pg} change with change in the valve coefficients at steady states while w_{iv} change only during the transient period. Flow through the injection valve is not affected at a steady state due to the fact that there is no net change in annulus gas implying that $w_{iv} = w_{gl}$ at steady state. The mass of gas in the annulus is also seen to vary with changes in C_{iv} as seen in Fig. 4.

The mass of gas in the annulus behaves similarly to P_a (Fig. 4(f) and Fig. 5(f)), hence no need to include it. It is expected that mixture density should respond to both a change in C_{iv} and C_{pc} but Fig. 4(c) shows no residual change with fault in C_{iv} while shows change with fault in C_{pc}. Fig. 4(d),(e) and Fig. 5(d),(e) all behave as expected, with each residual responding to change in the corresponding fault and unaffected by fault in other coefficients. We therefore limit the additional variables to two which are P_{wh} and P_a.

2.3 Gas Lift models.

The gas lift models presented here are adapted from [11]. The mass (differential equations):

$$\frac{dm_{ga}}{dt} = w_{gl} - w_{iv} \tag{2}$$

$$\frac{dm_{gt}}{dt} = w_{iv} + w_{rg} - w_{pg} \tag{3}$$

$$\frac{dm_{ot}}{dt} = w_{ro} - w_{po} \tag{4}$$

Flow rate:

$$w_{iv} = C_{iv}\sqrt{max(0, \rho_a(P_a - P_w)} \tag{5}$$

$$w_{pc} = C_{pc}\sqrt{max(0, \rho_w(P_{wh} - P_s)}\ f(u) \tag{6}$$

$$w_{pg} = \frac{\lambda}{\lambda + 1} w_{pc} \tag{7}$$

$$w_{po} = \frac{1}{\lambda + 1} w_{pc} \tag{8}$$

$$w_{ro} = C_r\sqrt{\rho_o(P_r - P_{bh})} \tag{9}$$

$$w_{rg} = GOR \tag{10}$$

The pressure:

$$P_a = \left(\frac{T_a R}{V_a M} + \frac{g}{A_a}\right) ga \tag{11}$$

$$P_{wh} = \frac{T_t R}{M}\left(\frac{m_{gt}}{V_t + V_{bh} - \frac{m_{ot}}{\rho_l}}\right) \tag{12}$$

$$P_w = P_{wh} + \frac{\left(m_{gt} + m_{ot} - \rho_{mV_{bh}}\right) g H_t}{V_t} \tag{13}$$

$$P_{bh} = P_w + \rho_m g H_{bh} \tag{14}$$

The density:

$$\rho_a = \frac{m_{ga} P_a}{T_a R} \tag{15}$$

$$\rho_m = \frac{m_{gt} + m_{ot} - \rho_o L_{bh} A_{bh}}{L_w A_w} \tag{16}$$

3 Results and Discussion

3.1 Residual Generation

The residual has been shown in Fig. 4 and Fig. 5 of section 2.2 to change in reaction to a fault. Fig. 7 shows the decision function for the residuals for a no-fault case. It is seen that at no fault, the function variation is very small hence no fault can be detected. When a fault is introduced, these functions change in response to the faults as shown later in section 3.3.

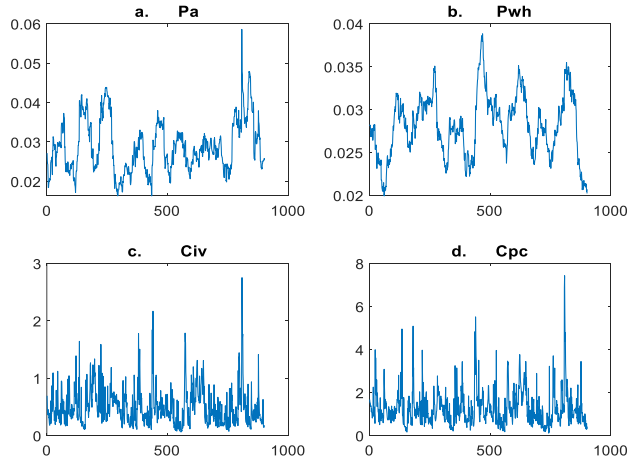

Fig. 7 No fault decision function based on the residuals

3.2 Hypothesis test using PDF data

ResidualS statistics of the gas lift system change following the arrival of fault. Fig. 8 is the PDF plot of the residual for the selected variables. The mean and standard deviation of some of the variables change with a fault when the production choke valve is increased by 20 % after the 600th minute. While for annulus pressure and wellhead pressure, the mean of the PDF shifts right following the fault, the PDF of the residual for the production choke characteristics shifts left after the fault, and that of the injection valve remains constant. The variation of the PDF of the residuals of some variables of the gas-lifted system with fault present is used to produce a decision function. This decision function is monitored which when an appropriate threshold is exceeded, a fault is detected, and the alarm rings.

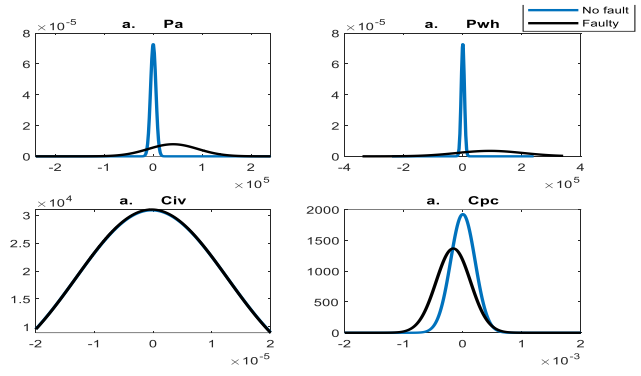

Fig. 8 PDF of the residuals for faulty and no-fault cases

The hypotheses according to [12], this hypothesis test is stated as follows:

H_0: $\Theta(i) = \Theta_0$ for $1 \leq i \leq t$

H_1: $\Theta(i) = \Theta_0$ for $1 \leq i \leq i_f$

$\Theta(i) = \Theta_1$ for $i_f \leq i \leq t$

Where i is the time instant, t is the simulation time and i_f is the fault occurrence time. We select H_0 if there is no change in decision function exceeding the selected threshold over the whole simulation time, else, H_1 is selected.

3.3 Fault detection using PDF data

The decision function for the fault of a 20 % increase in C_{iv} occurring at the 600th sample time is given in Fig. 9 while a 20 % increase in C_{pc} is given in Fig. 10. The data window is taken as N = 50 samples (minutes) and the simulation time is 1000 samples with the first 100 minutes removed to avoid the transient part (caused by the initial condition). In Fig. 9, only the annulus pressure P_a and C_{iv} decision function change in response to a fault. But in Fig. 10 the decision function corresponding to the annulus pressure, wellhead pressure and C_{pc} responded to the faults while the decision function for the C_{iv} does not respond to the C_{pc} fault.

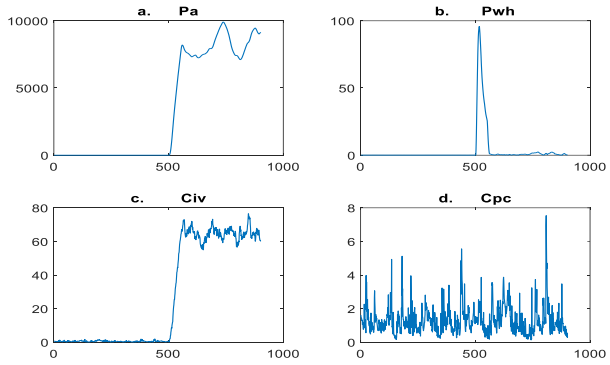

Fig. 9 Decision function for a fault of 20% in the C_{iv}

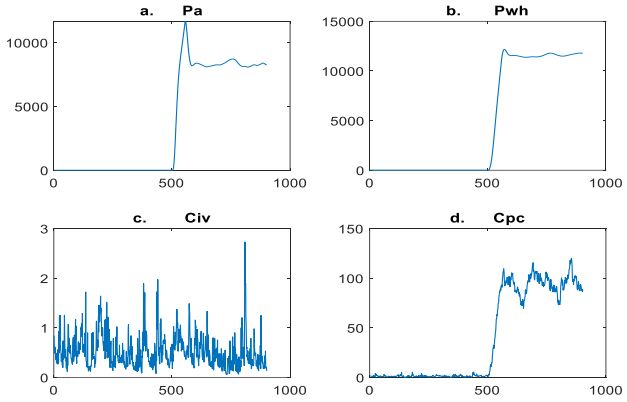

Fig. 10 Decision function for a fault of 20% in the C_{pc}

This makes it much easier to isolate faults in C_{pc} then it is for C_{iv}. Fig. 9 and Fig. 10 show that a threshold of h = 23 selected can easily be met with little detection delay. Fig. 11 and Fig. 12 show the zoomed sensitive residuals to indicate the point at which the fault is detected (time at which gk = h = 23) for Fig. 9 and Fig. 10 respectively, where gk implies decision function.

In Fig. 11 the gk for the P_a residual crossed h = 23 at 504 samples which is the detection time implying that the detection delay is therefore 3 samples, while the detection delay for the C_{iv} is 22 samples. Similarly, the detection delays in Fig. 12 are 3, 3, and 19 samples for P_a, P_{wh} and C_{pc} respectively. All these detection delays are within acceptable values for a gas lift system.

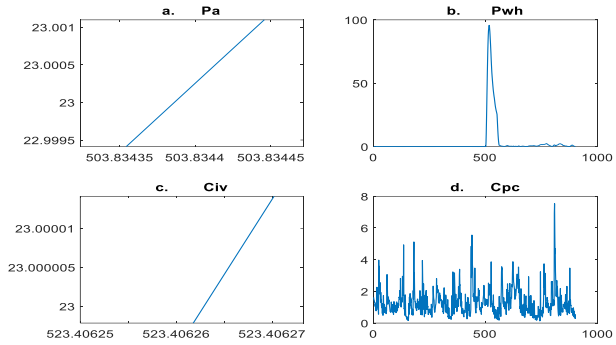

Fig. 11 Zoomed decision function for a fault of 20% in the C_{iv}

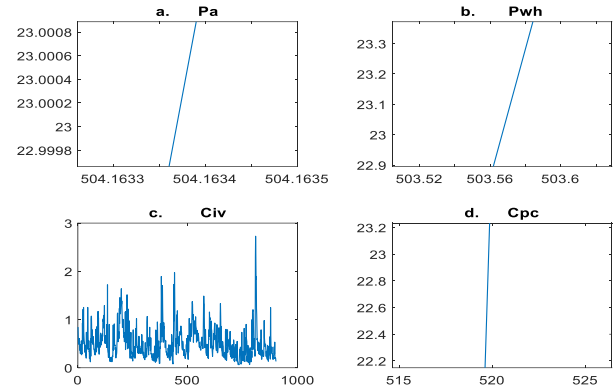

Fig. 12 Zoomed decision function for a fault of 20% in the C_{pc}

The estimated change magnitude of the parameter is 2.1*E-4 for C_{pc} and 5.7*E-5 for C_{iv}. If we note that C_{pc} provided is 2*E-3 and C_{iv} is 1E-4, then the estimated changed magnitude of the fault is 10 % for C_{pc} and 57 % for C_{iv}. But we apply a 20% change in both cases implying the effects of noise and the size of N has affected the estimated parameter at the point the fault is detected.

3.4 Fault isolation in gas lift system using PDF data.

For fault isolation, Table 1 shows the fault signatures for the variables and parameters selected. A 1 in the entry for a given residual implies the decision function changes following the arrival of the fault and 0 means the decision function is insensitive to a fault. From Table 1, each fault can be easily isolated since they have different signatures. The residual for the annulus pressure only helps in detection but not isolation as it is sensitive to both faults.

Table 1 Fault signatures for the gas lift system

	fault in C_{iv}	fault in C_{pc}
gk for P_a residual	1	1
gk for P_{wh} residual	0	1
gk for C_{iv} residual	1	0
gk for C_{pc} residual	0	1

The decision presented in Fig. 9 to Fig. 12 evaluates the residual and a simple logic is used to isolate the faults based on Table 1. The residual for P_a can be ignored as it is sensitive to both faults and a necessary condition for isolation is that the number of residuals must be at least equal to the number of faults. Even if P_a is removed, there are still three residuals for two faults.

4 Conclusion

Fault detection and isolation in the gas lift system was implemented considering the selected variables as stochastic hence the PDF data of these variables were used to generate fault signatures. The PDF data of the variables were used to generate decision functions used for both fault detection and isolation. The valve coefficients were used in addition to annulus pressure, flow through the injection valve, and pressure of the wellhead. The algorithm detected and isolated all fault scenarios examined for the gas lift system. The detection and isolation of the fault in the systems provide input to a fault-tolerant control system that ensures optimal operation of the gas lift system.

Conflict of interest

There is no conflict of interest in this article.

References

[1] Aamo, O.M., Eikrem, G.O., Siahaan, H.B. and Foss, B.A., 2005. Observer design for multiphase flow in vertical pipes with gas-lift—theory and experiments. *Journal of process control*, *15*(3), pp.247-257.

[2] Diehl, F.C., Almeida, C.S., Anzai, T.K., Gerevini, G., Neto, S.S., Von Meien, O.F., Campos, M.C., Farenzena, M. and Trierweiler, J.O., 2018. Oil production increase in unstable gas lift systems through nonlinear model predictive control. *Journal of Process Control*, *69*, pp.58-69.

[3] Eikrem, G.O., Aamo, O.M. and Foss, B.A., 2008. On instability in gas lift wells and schemes for stabilization by automatic control. *SPE Production & Operations*, *23*(02), pp.268-279.

[4] Eikrem, G.O., Foss, B., Imsland, L., Hu, B. and Golan, M., 2002. Stabilization of gas lifted wells. *IFAC Proceedings*, *35*(1), pp.139-144.

[5] Eikrem, G.O., Imsland, L. and Foss, B., 2004. Stabilization of gas lifted wells based on state estimation. IFAC Proceedings Volumes, 37(1), pp.323-328.

[6] Garcia, A.P., 2013, November. Stability analysis and stabilization of gas lift systems. In *22nd International Congress of Mechanical Engineering*, November (pp. 3-7).

[7] Jahanshahi, E., 2013. Control Solutions for Multiphase Flow: Linear and nonlinear approaches to anti-slug control. Norges teknisk-naturvitenskapelige universitet, Fakultet for naturvitenskap og teknologi, Institutt for kjemisk prosessteknologi.

[8] Scibilia, F., Hovd, M. and Bitmead, R.R., 2008. Stabilization of gas-lift oil wells using topside measurements. *IFAC Proceedings 41*(2), pp.13907-13912.

[9] Shi, J., Al-Durra, A., Errouissi, R. and Boiko, I., 2019. Stabilization of artificial gas-lift process using nonlinear predictive generalized minimum variance control. Journal of the Franklin Institute, 356(4), pp.2031-2059.

[10] Adukwu, O. and Oku, D.E., 2018. Modeling, Analysis and Monitoring DC Motor Using Proportional-Integral Controller and Kalman Filter. *Methodology*, *1*, p.2.

[11] Adukwu, O., Odloak, D., Saad, A.M. and Junior, F.K., 2022. State Estimation of Gas-Lifted Oil Well Using Nonlinear Filters. *Sensors*, *22*(13), p.4875.

[12] Basseville, M. and Nikiforov, I.V., 1993. Detection of abrupt changes: theory and application (Vol. 104). Englewood Cliffs: Prentice Hall.